Cell, Vol. 82, 453–461, August 11, 1995, Copyright © 1995 by Cell Press

DNA Strand Exchange Mediated by a RAD51-ssDNA Nucleoprotein Filament with Polarity Opposite to That of RecA

Patrick Sung* and Donald L. Robberson*†
*Sealy Center for Molecular Science
University of Texas Medical Branch at Galveston
Galveston, Texas 77555-1061
†Department of Molecular Genetics
University of Texas M. D. Anderson Cancer Center
Houston, Texas 77030

Summary

Yeast *RAD51* gene functions in genetic recombination and DNA double-strand break repair. In vitro, in the presence of ATP and replication protein A, RAD51 protein pairs single-stranded DNA (ssDNA) with homologous double-stranded DNA (dsDNA) and catalyzes strand exchange between the synapsed DNA partners. Electron microscopic analyses show that RAD51 forms helical filaments on both ssDNA and dsDNA, in which the DNA is highly extended. However, results presented here indicate that only the RAD51-ssDNA nucleoprotein filament is functionally relevant. Strand exchange is arrested when heterology is encountered in the duplex partner, and analysis of the configuration of the terminal joint thus formed reveals that pairing and strand exchange initiate at the 5′ end of the complementary strand in the linear duplex, a reaction polarity opposite to that of the bacterial prototype RecA.

Introduction

The *RAD51* gene of Saccharomyces cerevisiae is a member of the *RAD52* epistasis group that is required for genetic recombination and for DNA double-strand break repair (reviewed by Petes et al., 1991). Mutational inactivation of *RAD51* results in extreme cellular sensitivity to ionizing radiation and alkylating agents and in defects in spontaneous and DNA damage-induced mitotic recombination, as well as in meiotic recombination (Petes et al., 1991; Shinohara et al., 1992). The efficiency of spore formation and the spore viability are also affected adversely in *rad51* mutants (Petes et al., 1991; Shinohara et al., 1992), a phenotype consistent with the requirement for *RAD51* in meiotic recombination (Petes et al., 1991).

The measurement of spore viability of recombination defective mutants in the *spo13* genetic background has been a useful approach for determining whether a mutant is blocked at an early or a later step in the recombination process. Since the *spo13* mutation bypasses the reductional division that occurs during meiosis, formation of viable spores is possible even in the absence of the initiation of genetic exchange, because chromosomal nondisjunction associated with a recombination defect is prevented in the *spo13* mutant. However, the spore inviability in *rad51* mutants is not rescued by the *spo13* mutation, indicating that the *RAD51* function is required in genetic recombination subsequent to the initiation step (reviewed by Petes et al., 1991).

The yeast *RAD51* gene was isolated independently by three different groups (Aboussekhra et al., 1992; Basile et al., 1992; Shinohara et al., 1992), and the *RAD51* counterparts from various mammalian sources have also been cloned. The structure of the RAD51 protein is highly conserved among eukaryotes, and the human RAD51 homolog exhibits 67% identity to the yeast counterpart (Shinohara et al., 1993; Yoshimura et al., 1993). Importantly, yeast RAD51 (M_r, 43,000) and its counterparts from higher eukaryotes possess highly significant sequence similarity to the Escherichia coli RecA protein (Aboussekhra et al., 1992; Basile et al., 1992; Shinohara et al., 1992, 1993; Yoshimura et al., 1993). Between yeast RAD51 and RecA, the homology is localized to the middle portion of the two proteins, encompassing ~220 amino acid residues, wherein ~30% of the residues are identical (Aboussekhra et al., 1992; Basile et al., 1992; Shinohara et al., 1992). RecA protein (M_r, 37,800) plays a central role in genetic recombination and DNA repair in E. coli via its ability to mediate pairing and strand exchange between homologous DNA molecules. RecA is a DNA-dependent ATPase, and in the presence of ATP or an ATP analog, it polymerizes on both single-stranded DNA (ssDNA) and double-stranded DNA (dsDNA) to form highly ordered, right-handed helical filaments. These nucleoprotein filaments have a helical pitch of ~95 Å, and the DNA is extended by ~50% relative to a naked B-form duplex (reviewed by Griffith and Harris, 1988; Radding, 1991; Roca and Cox, 1990). In the model in vitro system with circular viral ssDNA and homologous linear dsDNA, pairing of the DNA substrates is mediated by the RecA filament on the ssDNA. In the strand exchange phase, the complementary strand in the linear duplex is transferred unidirectionally, beginning from its 3′ terminus, onto the ssDNA bound in the RecA filament, resulting in the creation of heteroduplex DNA within the filament (reviewed by Griffith and Harris, 1988; Kowalczykowski et al., 1994; Radding, 1991; Roca and Cox, 1990).

Recently, we have purified RAD51 protein to near homogeneity from a S. cerevisiae strain genetically tailored to overproduce the protein and have shown that RAD51 catalyzes homologous DNA pairing and strand exchange. The pairing and strand exchange reaction shows a strict dependence on ATP, consistent with the presence of a ssDNA-dependent ATPase in RAD51 (Sung, 1994). To begin defining the molecular mechanisms of the RAD51 catalyzed DNA pairing and strand exchange reaction, we now examine the interaction of RAD51 protein with DNA. We show here that RAD51 forms helical filaments on not only dsDNA, as reported by Ogawa et al. (1993), but also on ssDNA in an ATP-dependent manner and that the DNA in the RAD51 filaments is in an extended conformation. Importantly, our results indicate that while formation of

RAD51–ssDNA nucleoprotein filament leads to pairing and strand exchange, the RAD51 filament on dsDNA is not only incapable of initiating pairing and strand exchange, but is in fact strongly inhibitory to these reactions. Interestingly, we find that the RAD51 catalyzed pairing and strand exchange reaction has a polarity opposite to that of RecA.

Results

ATP-Dependent Pairing and Strand Exchange

For studying the mechanistic aspects of RAD51-catalyzed homologous DNA pairing and strand exchange, the RAD51 protein was purified to near homogeneity from a yeast strain that overproduces the protein (Sung, 1994). The ssDNA-binding protein replication protein A (RPA), a heterotrimer of 69 kDa, 36 kDa, and 13 kDa subunits, was also purified from yeast extract to near homogeneity as described elsewhere (Brill and Stillman, 1989).

In the standard pairing and strand exchange reaction, circular ssDNA from the bacteriophage ΦX174 is incubated with RAD51 protein at a ratio of one protein monomer to ~2.9 nt of DNA in the presence of ATP, followed by the addition of RPA and a brief incubation, and then linear ΦX174 dsDNA is added (see Experimental Procedures). The reaction products, the joint molecule and nicked circular duplex, are resolved by agarose gel electrophoresis and visualized by staining with ethidium bromide (Figure 1A). The kinetics of formation of the two reaction products are presented in Figure 1B. After 120 min of reaction, the majority (82%) of the input linear dsDNA was in the form of either joint molecule (22%) or nicked circular duplex (60%).

RAD51 protein possesses a ssDNA-dependent ATPase activity (Sung, 1994). Importantly, pairing and strand exchange do not occur in the absence of ATP (Figure 1A, lane 8; Sung, 1994). RPA serves an important accessory role, as its omission causes a marked reduction in the formation of joint molecule and of nicked circular duplex characteristic of complete strand exchange (Sung, 1994; P. S., unpublished data).

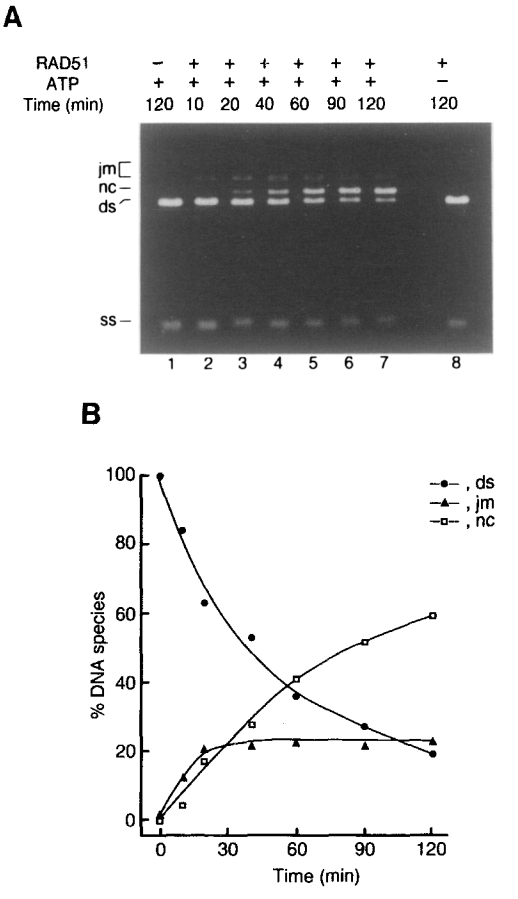

Figure 1. Homologous Pairing and Strand Exchange

(A) Reaction mixtures containing ΦX linear dsDNA and ΦX circular (+) strand that had been pretreated with RAD51 and RPA were incubated at 37°C for the indicated times. The input DNA substrates and the reaction products (joint molecules and nicked circular duplex) were resolved in a 0.9% agarose gel and visualized by staining with ethidium bromide. Abbreviations: jm, joint molecules; nc, nicked circular duplex; ds, linear duplex; ss, circular (+) strand. Note that joint molecules and nicked circular dsDNA were not formed when ATP was absent (lane 8).

(B) The gel shown in (A) was subjected to image analysis to obtain datapoints for a graphical representation of the results.

Nucleoprotein Filament Formation

A previous study described the ATP-dependent formation of RAD51 protein filament on dsDNA (Ogawa et al., 1993). Since pairing and strand exchange occur efficiently with precoating of ssDNA with RAD51, as is done in our standard experimental protocol (see Figure 1; Experimental Procedures), we wished to determine the nature of the complex of RAD51 protein with ssDNA. To do this, we incubated ΦX174 viral (+) strand with RAD51 protein and RPA under the same set of buffer and reaction conditions employed in the pairing and strand exchange assay, and, without any fixative treatment, the reaction samples were applied to polylysine-coated grids in preparation for examination by electron microscopy. Nucleoprotein filaments with a highly regular, right-handed helical appearance were observed upon incubation of RAD51 protein with the viral (+) strand in the presence of ATP and RPA (Figure 2A). The nucleoprotein filaments were abundant, suggesting that they were the major type of protein–DNA complex formed. Importantly, nucleoprotein filaments were not formed when ATP was omitted (data not shown), indicating that, as for pairing and strand exchange, polymerization of RAD51 protein on the ssDNA requires ATP. The nucleoprotein filaments have a mean helical pitch of 96 Å, as derived from averaging 21 data sets. Results from examining 32 DNA molecules fully coated with RAD51 protein by a combination of negative staining and shadowing revealed that the nucleoprotein filaments have a mean contour length of 2.77 μm. Since duplex ΦX174 DNA (5386 bp) in the B form is expected to have a contour length of 1.8 μm, the length of the ssDNA in the nucleoprotein filament is ~154% that of a B-form duplex. This increased length corresponds to an axial rise of ~18.6 bases of ssDNA per helical repeat of the nucleoprotein filament. When the

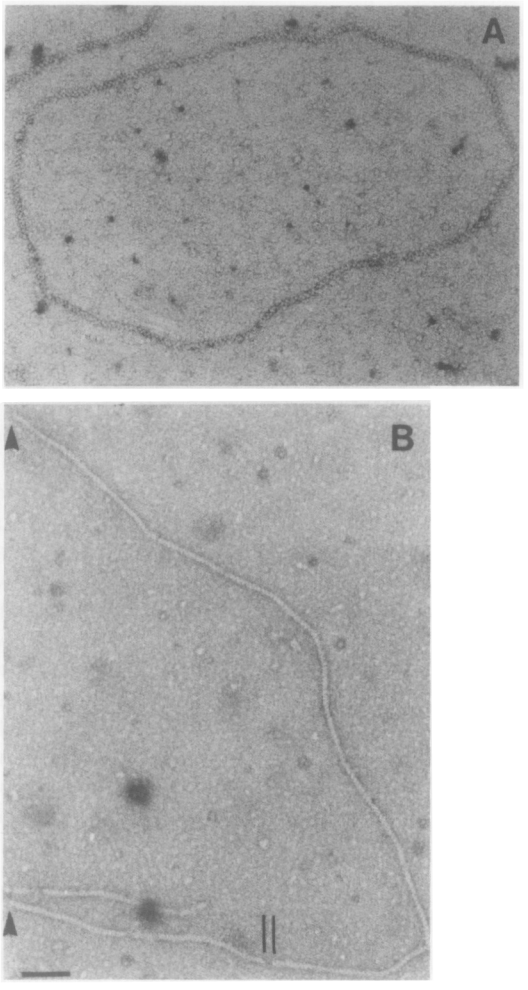

Figure 2. RAD51 Filaments Formed on ssDNA and dsDNA

Electron micrographs of a representative RAD51 filament formed on ΦX174 viral (+) strand in the presence of RPA (A) and on linear ΦX174 duplex, with the DNA termini indicated by arrowheads (B). Nucleoprotein filaments appear as right-handed helices. The two parallel vertical lines in (B) point to a gap in the nucleoprotein filament. RAD51 filaments were not formed on ssDNA and dsDNA in the absence of ATP (data not shown). The samples were negatively stained with 1% uranyl acetate, and the magnification is indicated by the bar length of 100 nm located in the lower left corner of (B).

ssDNA was incubated with RAD51 protein in the absence of RPA, nucleoprotein filaments were again formed in an ATP-dependent fashion (data not shown). However, the covering of ssDNA by RAD51 protein was typically less contiguous than in the presence of RPA, indicating that RPA facilitates the polymerization of RAD51 protein on ssDNA, probably by removing secondary structure in the DNA.

In confirmation of the results of Ogawa et al. (1993), we also observed ATP-dependent formation of RAD51 filaments on dsDNA (Figure 2B). RAD51 filament formed on linear ΦX dsDNA has a right-handed helicity, a pitch of 80 Å (average of 24 data sets), and a mean contour length of 2.44 μm (20 molecules measured), indicating that the DNA is extended to ~135% of the B-form length, corresponding to an axial rise of ~17.6 bp per helical repeat of the nucleoprotein filament.

Although RAD51 forms filaments on both dsDNA and ssDNA, results presented below demonstrate a striking difference in the relevance of the two species of nucleoprotein filaments to pairing and strand exchange.

dsDNA in RAD51 Filament Cannot Pair with ssDNA

Results presented thus far indicate that formation of RAD51 filament on ssDNA leads to pairing and strand exchange. We also examined whether homologous pairing could be mediated via RAD51 filament formation on dsDNA. To do this, we incubated dsDNA with RAD51 protein to form nucleoprotein filament and mixed the RAD51 protein–dsDNA filament with uncoated ssDNA and RPA. However, there was no evidence of pairing even after 120 min of incubation (data not shown), thus indicating that the RAD51 protein–dsDNA filament is incapable of initiating the pairing reaction.

Upon examining the effect of varying the ratio of RAD51 protein to ssDNA on pairing and strand exchange with the duplex partner, it was observed that the extent of reaction diminished abruptly when RAD51 protein was used in excess of the optimal ratio of one protein monomer to 2.7–3.2 nt of ssDNA (Figure 3A). For instance, increasing the RAD51 protein amount in the standard reaction so that the ssDNA nucleotide to protein monomer ratio fell from 2.7 to 1.5 and 0.8 actually resulted in 67% and 89% inhibition of product formation, respectively (Figure 3B). One possible explanation for this phenomenon is that coating of the subsequently added dsDNA by free RAD51 protein present in excess of what is needed to coat the ssDNA sequesters the dsDNA and inhibits the pairing between the DNA partners. This hypothesis is consistent with the observation that in the case in which dsDNA was first coated with RAD51 protein, even at RAD51 concentrations at which there should be sufficient free protein to coat the subsequently added ssDNA as well, pairing still did not occur (data not shown).

To test directly the effect of coating the dsDNA with RAD51 protein on pairing with RAD51–ssDNA filament, we conducted the following two experiments. In the first experiment, preformed RAD51–ssDNA filament was mixed with dsDNA that had been coated separately with increasing concentrations of RAD51 protein, and the amount of reaction products obtained was compared with that formed when the RAD51–ssDNA filament was reacted with naked dsDNA. As shown in Figure 4A, coating of the dsDNA with RAD51 protein proved to be strongly inhibitory to pairing and strand exchange, such that when the dsDNA was preincubated with RAD51 protein at ratios of 7, 4, and 2 bp per protein monomer, the amount of reaction products observed was reduced to 71%, 32%, and 3%, respectively, of that observed with the naked dsDNA control after 90 min of incubation.

In the second experiment, the ability of naked dsDNA versus RAD51 coated dsDNA to pair with the RAD51–ssDNA filament was compared. To do this, we included

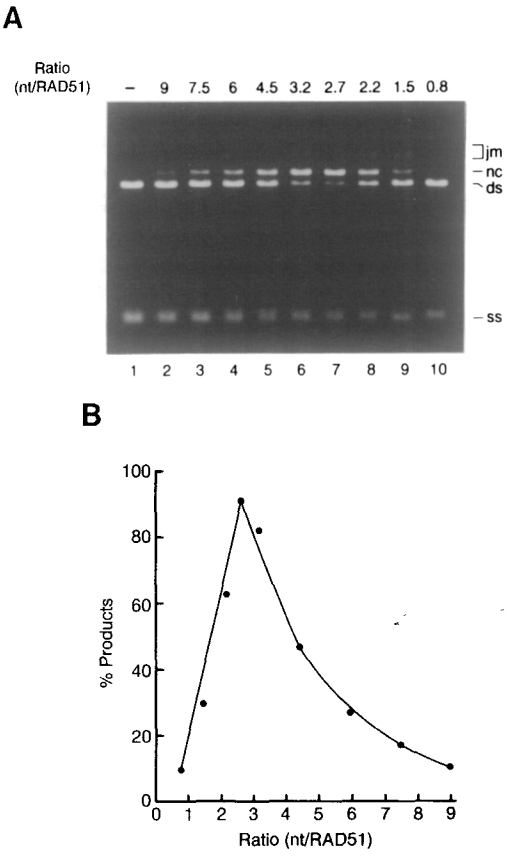

Figure 3. Pairing and Strand Exchange as a Function of RAD51 Amount

(A) Circular ΦX (+) strand DNA was preincubated with RPA and varying amounts of RAD51 protein added in 1.2 μl to give the indicated ratios of nucleotides (nt) per RAD51 monomer. Following the incorporation of linear dsDNA, the reaction mixtures were incubated at 37°C for 120 min, deproteinized, and subjected to electrophoresis in a 0.9% agarose gel, which was treated with ethidium bromide to stain the DNA species. The reaction volume and the concentration of RPA and DNA substrates were as described under the standard protocol in Experimental Procedures.

(B) Graphical representation of the results in (A). Abbreviations: jm, joint molecules; nc, nicked circular duplex; ds, linear duplex; ss, circular (+) strand.

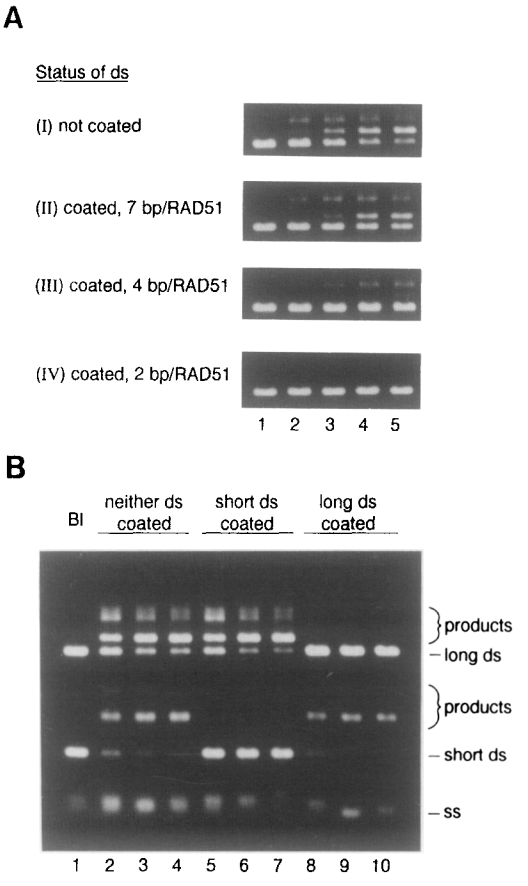

Figure 4. Coating of dsDNA by RAD51 Inhibits Pairing

(A) Linear ΦX dsDNA, precoated with increasing RAD51 amounts (II–IV), was reacted with the RAD51–ssDNA filament for 20, 40, 60, and 90 min (lanes 2, 3, 4, and 5, respectively). In lane 1, the DNA substrates were incubated for 90 min in buffer without RAD51 protein.

(B) Either the full-length linear ΦX dsDNA, designated as long ds, or a 2.9 kb fragment derived from it, designated as short ds, was precoated with RAD51 protein at 2.5 bp per protein monomer before being reacted with RAD51–ssDNA filament at 37°C for 45 min (lanes 5 and 8), 90 min (lanes 6 and 9), and 120 min (lanes 7 and 10). The full-length linear ΦX dsDNA and short dsDNA, neither of which was coated with RAD51, were also incubated with RAD51–ssDNA filament at 37°C for 45 min (lane 2), 90 min (lane 3), and 120 min (lane 4). Abbreviations: ss, viral circular (+) strand; BI, DNAs incubated in buffer without RAD51 for 120 min. The joint molecules and products of complete strand exchange are marked collectively as products; the upper set of products resulted from the reaction between the long dsDNA and the circular (+) strand, and the lower set of products were derived from the short dsDNA and the circular (+) strand. The details are given in Experimental Procedures.

in the same reaction mixture a 2.9 kb fragment derived from the full-length duplex, besides the linear ΦX duplex that is 5.38 kb in size (see Experimental Procedures). As shown in Figure 4B, the pairing and strand exchange products formed between the RAD51–ssDNA filament with the shorter duplex are well resolved from those formed with the full-length duplex in an agarose gel, thus allowing us to determine the effect of precoating either the full-length or the shorter duplex with RAD51 on its ability to participate in pairing and strand exchange. We found that precoating of either duplex with RAD51 at 2.5 bp per protein monomer greatly diminished the ability of that duplex to participate in the pairing reaction; however, it also revealed that the coating of either duplex with RAD51 protein did not affect the ability of the uncoated counterpart to pair with the RAD51–ssDNA filament.

Region of Heterology in the Duplex Partner Halts Branch Migration

When the input DNA substrates were the viral single-stranded circle and the linear double-stranded form of M13 DNA, RAD51 protein also catalyzed the pairing and strand exchange between these partners (Sung, 1994; Figure 5, lanes 1–4). In this case, although pairing occurred efficiently, conversion of the joint molecule to the complete strand exchange product, the nicked circular duplex, was lower than that obtained with the ΦX174 substrates. For

instance, after 80 min and 120 min of incubation, 10% and 18%, respectively, of the M13 linear duplex (7.25 kb) had been converted to nicked circular duplex (Figure 5, lanes 3 and 4), which was considerably less than the >50% conversion of linear ΦX174 duplex (5.38 kb) to the nicked circular duplex form after 90 min of reaction (see Figure 1). The lower efficiency of conversion of the M13 duplex to the full exchange product compared with the ΦX duplex may reflect the presence of structural impediments in the M13 DNA.

The introduction of an unrelated DNA sequence into the polylinker region of the M13 molecule enabled us to test the effect of a heterologous sequence in the linear duplex on pairing and strand exchange. The M13 hybrid that contains the 458 bp heterologous insert, which is designated h.M13.1, was linearized at the unique BspHI site. In the linear form, the region of heterology is located at ~2.2 kb from the 5′ end of the (−) strand. As shown in Figure 5 (lanes 6–9), when the h.M13.1 duplex was incubated with RAD51 coated ss circle from M13 without the insert, the joint molecule was formed readily, but product with mobility expected of nicked circular duplex was not detected. However, nicked circular duplex was generated from linear h.M13.1 duplex if the input single-stranded circular DNA was also derived from the h.M13.1 phage (Figure 5, lanes 10–13). Taken together, these results indicate that the presence of a region of heterology of 458 bp in the linear duplex partner arrests the branch migration reaction.

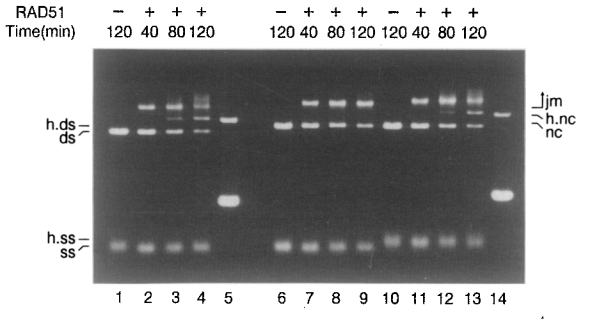

Figure 5. Branch Migration Is Halted by Heterology

Circular M13mp18 or h.M13.1 (+) strand was coated with RAD51 and RPA as described in the standard protocol and then incubated with linear M13mp18 or h.M13.1 dsDNA at 37°C for the indicated times. Abbreviations for the input DNA substrates: ss, circular M13mp18 (+) strand; h.ss, circular h.M13.1 (+) strand; ds, linear M13mp18 duplex; h.ds, linear h.M13.1 duplex. DNA substrates: lanes 1–4, ssDNA and dsDNA; lanes 6–9, ssDNA and h.M13.1 dsDNA; lanes 10–13, h.M13.1 ssDNA and h.M13.1 dsDNA. Abbreviations for the reaction products: nc, nicked circular M13mp18 duplex, formed as a result of complete strand exchange between ssDNA and dsDNA; h.nc, nicked circular h.M13.1 duplex, formed as a result of complete strand exchange between h.M13.1 ssDNA and h.M13.1 dsDNA; jm, joint molecules formed by pairing either ssDNA or h.M13.1 ssDNA with either dsDNA or h.M13.1 dsDNA. Lane 5 contains replicative form M13mp18 DNA consisting of a mixture of nicked circular (upper band) and supercoiled (lower band) species, and lane 14 contains replicative form h.M13.1 DNA consisting of a mixture of nicked circular (upper band) and supercoiled (lower band) species. For clarity, the positions of the supercoiled species in lanes 5 and 14 are not marked.

Polarity of Pairing and Strand Exchange

On the assumption that the RAD51-catalyzed pairing and strand exchange would have a unique polarity, it could be predicted that the terminal joint formed between M13 ssDNA and the h.M13.1 linear duplex would be in either of the two possible configurations depicted in Figure 6A. These configurations can be distinguished by restriction analyses, as explained in the legend to Figure 6.

To determine the polarity of the RAD51-promoted pairing and strand exchange reaction, we 5′-end labeled the linear h.M13.1 duplex with ^{32}P and incubated it with RAD51–M13 ssDNA filament. At 40, 80, and 120 min, a portion of the reaction mixture was digested with either the restriction enzyme ClaI or XmnI, followed by deproteinization with SDS and proteinase K. Samples were subjected to electrophoresis in agarose gels, which were dried and exposed to X-ray films to visualize the pattern of digestion. Figure 6B shows that when the restriction enzyme used was ClaI, a 1.2 kb fragment and a 1.6 kb fragment were formed in the absence of RAD51 protein (lane 1). During the pairing and strand exchange reaction, a time-dependent disappearance of the 1.6 kb fragment was observed, while the amount of the 1.2 kb fragment remained essentially constant throughout (Figure 6B, lanes 2–4). Generation of this unique restriction pattern was dependent upon the presence of ATP in the reaction, as, when ATP was omitted, the amount of the 1.6 kb ClaI fragment generated was indistinguishable from the minus RAD51 control (Figure 6B, lane 5). As illustrated in Figure 6A, this restriction pattern obtained with ClaI indicates that RAD51 catalyzed pairing initiates at the 5′ end of the (−) strand in the linear duplex.

To verify this reaction polarity further, we subjected the pairing and strand exchange reaction mixture to restriction with XmnI (Figure 6C), which yielded a 0.9 kb fragment and a 1.3 kb fragment in the minus RAD51 control (lane 1). In this case, concomitant with pairing and strand exchange, the smaller (0.9 kb) fragment disappeared in an ATP-dependent fashion (Figure 6C, lanes 2–5), which again indicated that the RAD51-catalyzed pairing and strand exchange reaction initiates at the 5′ terminus of the (−) strand in the linear duplex.

We have also used this system to examine the reaction polarity of E. coli RecA protein, and as expected (for references see Radding, 1991), we observed that the 3′ end of the (−) strand in the linear duplex is used preferentially by RecA for pairing and strand exchange (data not shown). Thus, the reaction polarity of RAD51 is opposite to that of RecA. The Rec1 protein of Ustilago maydis has also been shown to catalyze DNA strand exchange with a polarity opposite to that of RecA (Kmiec and Holloman, 1983).

Discussion

Role of RAD51 Nucleoprotein Filament in Pairing and Strand Exchange

Results from several experiments conducted in the present study show that preincubation of RAD51 protein with ssDNA in the presence of RPA leads to efficient pairing and strand exchange with the uncoated double-stranded

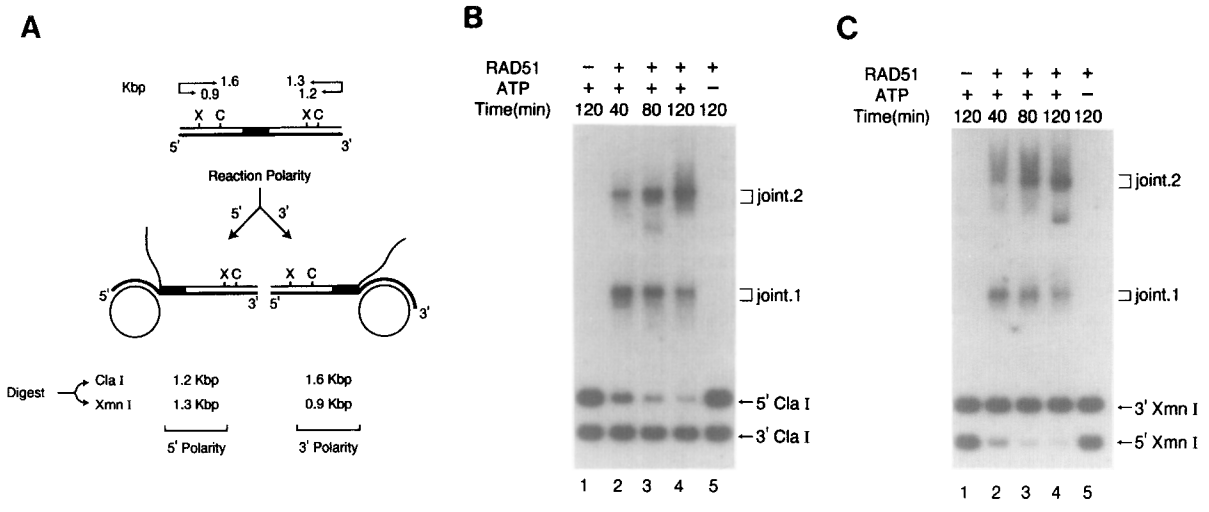

Figure 6. Pairing and Strand Exchange Initiate at the 5′ End of the Linear Duplex

(A) The experimental design. Replicative form h.M13.1 DNA was linearized at the unique BspHI site, and the 5′ termini were labeled with ^{32}P. In the linear dsDNA form of h.M13.1, the 458 bp heterologous insert, designated by the closed region, is located 2.2 kb from the 5′ end of the (−) strand, which is designated by the thicker line. Pairing of the (−) strand in the duplex with the viral (+) strand will initiate from either the 3′ or the 5′ end of the former, and thereafter branch migration will proceed until it is blocked by the heterologous insert. The two possible configurations of the terminal complex depicted can be distinguished by treating the reaction mixture with the restriction enzymes ClaI and XmnI. The unreacted duplex will yield radiolabeled fragments of 1.2 kb and 1.6 kb when digested with ClaI and will yield radiolabeled fragments of 0.9 kb and 1.3 kb when digested with XmnI. If the 5′ end of the (−) strand is used for pairing, the intensity of the 1.2 kb ClaI fragment and the 1.3 kb XmnI fragment will remain unchanged, whereas the intensity of the 1.6 kb ClaI fragment and the 0.9 kb XmnI fragment will diminish as pairing and strand exchange progress. However, if the 3′ end of the (−) strand is used in pairing, a pattern opposite to that just described would be seen.

(B and C) The 5′ end of the (−) strand in the linear duplex is used. Linear h.M13.1 dsDNA ^{32}P-labeled at the 5′ end was reacted with M13 viral (+) strand coated with RAD51 protein and RPA, and at 40, 80, and 120 min (lanes 2–4), a portion of the reaction mixture was digested with ClaI (B) or XmnI (C). In lane 5, the radiolabeled linear h.M13.1 dsDNA was incubated with M13 (+) strand, RAD51, and RPA in the absence of ATP for 120 min and then digested with ClaI (B) or XmnI (C). In lane 1, the radiolabeled linear h.M13.1 dsDNA and M13 viral (+) strand were incubated in the presence of ATP, but without RAD51 and RPA, for 120 min and then digested with either ClaI (B) or XmnI (C). Following electrophoresis in an agarose gel, autoradiography revealed radiolabeled DNA species. Abbreviations: 5′ ClaI and 3′ ClaI in (B), the ClaI fragments that contain the 5′ end and the 3′ end of the (−) strand of the linear duplex, respectively; 5′ XmnI and 3′ XmnI in (C), the XmnI fragments that contain the 5′ end and the 3′ end of the (−) strand of the linear duplex, respectively; joint.1, the joint molecule of M13 viral (+) strand and the ClaI fragment (B) or XmnI fragment (C) containing the radiolabeled 5′ end of the (−) strand, which was formed because branch migration had not proceeded past the 5′ ClaI and 5′ XmnI sites at the time of digestion with the restriction enzymes; joint.2, the joint molecule of viral (+) strand and the remainder of the radiolabeled linear h. M13.1 dsDNA after removal of the ClaI fragment (B) or XmnI fragment (C) that contained the 3′ end of the (−) strand.

partner, whereas precoating of dsDNA with RAD51 protein precludes its participation in pairing with naked ssDNA or with RAD51-coated ssDNA. During pairing and strand exchange, an amount of RAD51 corresponding to one protein monomer to ~3 nt of ssDNA is required for obtaining the optimal reaction rate. Taken together, our results indicate that RAD51-catalyzed pairing and strand exchange is mediated by a stoichiometric complex of RAD51 protein on ssDNA. By electron microscopy, we observed that RAD51 protein forms right-handed helical filaments not only on dsDNA, as has been reported by Ogawa et al. (1993), but on ssDNA as well. The biochemical data presented herein establish that the RAD51 filament on dsDNA is biologically inactive, while several lines of evidence strongly suggest that pairing and strand exchange occur within the RAD51–ssDNA nucleoprotein filament. First, as noted above, our results indicate that pairing and strand exchange are effected via a stoichiometric complex of RAD51 on ssDNA. Second, both the formation of nucleoprotein filament and pairing share a common requirement for ATP, which is consistent with the notion that polymerization of RAD51 protein on ssDNA leads to pairing and strand exchange. Third, the single-stranded DNA-binding protein RPA, which is an important accessory factor in pairing and strand exchange, stimulates nucleoprotein filament formation, providing a direct correlation between the extent of RAD51 polymerization on ssDNA and the efficiency of ensuing pairing and strand exchange. Thus, it appears that pairing and strand exchange catalyzed by RAD51 protein also occurs within the confines of a nucleoprotein filament, just as it does in RecA (Griffith and Harris, 1988; Kowalczykowski et al., 1994; Radding, 1991; Roca and Cox, 1990). We have incorporated the results from the biochemical and electron microscopic analyses into a working model for RAD51 action, as shown in Figure 7.

Mechanistic and Structural Distinctions between RAD51 and RecA

Aside from the many structural and functional parallels shared by RecA and RAD51, there also exist notable differences between these two recombinases. Catalytically, under conditions that are optimal for pairing and strand exchange, RAD51 protein hydrolyzes ATP at ~2% the rate measured for RecA protein (Sung, 1994; P. S., unpublished data), which may very well reflect an important mechanistic difference in the manner ATP is utilized by

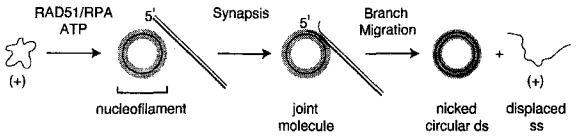

Figure 7. RAD51 Reaction Mechanism

In the presence of RPA and ATP, RAD51 protein polymerizes on the circular (+) strand to form nucleofilament. The model postulates that synapsis between the circular (+) strand and the homologous linear double-stranded partner occurs within the context of the nucleofilament. Our results indicate that the 5′ end of the (−) strand in the linear duplex is used in pairing with the viral (+) strand. Following synapsis, unidirectional branch migration yields nicked circular duplex and linear (+) strand as products.

the two proteins when catalyzing pairing and strand exchange. Our results have further demonstrated that the 5′ end of the duplex partner is utilized by the RAD51–ssDNA filament for pairing and strand exchange, a reaction polarity that is opposite to that of RecA.

Structurally, the homology between RecA and RAD51 is restricted to the middle portions of the two proteins spanning ~220 residues, wherein there is ~30% identity (Aboussekhra et al., 1992; Basile et al., 1992; Shinohara et al., 1992). Outside of this homologous core, however, the two proteins differ considerably, as RAD51 bears an N-terminal extension of ~120 residues not present in RecA but is shorter than RecA protein by ~90 residues at the C-terminus (Aboussekhra et al., 1992; Basile et al., 1992; Shinohara et al., 1992). Furthermore, between residues 296 and 317 in RAD51 protein, we have noted the sequence L-X_6-L-X_6-L-X_6-F, which resembles the leucine zipper motif that mediates protein–protein interactions and which is absent in RecA protein. These structural distinctions could account for the differences in action mechanism between RecA and RAD51 and could also reflect the sets of evolutionarily diverged recombination proteins that RAD51 and RecA need to interact with in accomplishing their respective biological roles.

Implications for RAD51 Homologs

The *RAD51* structure and function have been conserved strongly throughout evolution, since homologs of *RAD51* have been described in a variety of eukaryotic organisms including mouse, chicken, and human (Bezzubova et al., 1993; Morita et al., 1993; Shinohara et al., 1993; Yoshimura et al., 1993). All these homologs exhibit remarkable amino acid sequence identity (>60%) to S. cerevisiae RAD51 protein. Furthermore, expression of the mouse RAD51 counterpart in a S. cerevisiae *rad51* mutant complements the DNA repair defect of the mutant, indicating functional conservation (Morita et al., 1993). The structural and functional conservation makes it highly probable that the RAD51 homologs from these and other eukaryotic organisms also catalyze ATP-dependent homologous pairing and strand exchange via a similar mechanism.

The S. cerevisiae *DMC1*-encoded product and RAD51 share 45% identical residues over the entire length of the two proteins (Bishop et al., 1992; Shinohara et al., 1992), strongly suggesting that, like RAD51, the DMC1 protein also has ATP-dependent homologous pairing and strand exchange activities. *DMC1* is expressed only during meiosis, and the *dmc1* null mutant shows no discernible mitotic phenotype but exhibits severe meiotic abnormalities, including an arrest in prophase, failure to form normal synaptonemal complex, and a defect in genetic recombination (Bishop et al., 1992; Bishop, 1994). In meiosis, DMC1 protein may act as an alternate to RAD51 in catalyzing pairing and strand exchange. The middle portion of the proteins encoded by S. cerevisiae *RAD55* and *RAD57* genes, which are both members of the *RAD52* group, exhibit homology to RAD51 (Basile et al., 1992; Lovett, 1994), suggesting that they, too, may have some or all of the enzymatic activities that we have described for RAD51. Thus, RAD55 and RAD57 could function with RAD51 in pairing and strand exchange in vivo to ensure a high efficiency of genetic recombination and DNA strand break repair. However, since the radiation sensitivity of *rad55* and *rad57* null mutants can be suppressed by increased temperature and osmotic strength, as well as by heterozygosity at the mating-type locus (Lovett and Mortimer, 1987), it seems likely that the putative recombination activity of RAD55 and RAD57 proteins is supplementary to the RAD51 function.

Recombination In Vivo

Characterization of chromosomal sites that have a notable propensity to undergo meiotic recombination has revealed the formation of meiosis-specific double-strand breaks at these sites (Cao et al., 1990; Sun et al., 1989). As has been observed in Southern blot analyses with the use of strand-specific probes, upon formation of the double-strand breaks, 5′ to 3′ exonucleolytic resection yields 3′ single-stranded tails of considerable lengths (Cao et al., 1990; Sun et al., 1991). Accumulated evidence strongly suggests that the 3′ single-stranded region that results from the exonucleolytic processing of double-strand breaks represents the immediate precursor that effects pairing with the homologous double-stranded partner. In vivo, nucleation of RAD51 protein on the 3′ single-stranded region with the aid of RPA and possibly other *RAD52* group proteins will lead to homology search and pairing with the intact homolog, resulting in the joining of the homologous chromosomes involved and an exchange of genetic information between them. It may be envisioned that the repair of double-strand breaks induced by DNA damaging treatment would follow the same mechanistic route as recombination initiated from meiotic double-strand breaks, since both processes have the same requirement for *RAD51* and other members of the *RAD52* group.

Experimental Procedures

Proteins

RAD51 protein was purified to near homogeneity from extract of the yeast strain LP2749-9B harboring plasmid pR51.1 containing the *RAD51* gene under the control of the yeast alcohol dehydrogenase I promoter, as described previously (Sung, 1994). The procedure of Brill and Stillman (1989) was used to purify RPA to near homogeneity from extract of LP2749-9B. The RAD51 protein was stored in 10 mM KH_2PO_4 (pH 7.4) containing 10% glycerol, 350 mM KCl, 0.5 mM EDTA, and 0.5 mM DTT. RPA was stored in 25 mM Tris–HCl (pH 7.5), 10% glycerol, 1 mM EDTA, 1 mM DTT, and 100 mM NaCl.

DNA Substrates

The replicative form and the circular viral (+) strand of ΦX174 DNA were purchased from GIBCO BRL. The circular viral (+) strand of M13mp18 and that of h.M13.1 were purified from phage-infected E. coli culture supernatants by polyethylene glycol precipitation followed by two rounds of cesium chloride banding. Replicative form M13mp18 DNA and h.M13.1 DNA were purified by two rounds of cesium chloride banding after alkaline lysis of infected E. coli cells. h.M13.1 is M13mp18 containing a 458 bp EcoRI–HindIII fragment derived from the *RAD54* gene (Emery et al., 1991). Replicative form ΦX DNA was linearized by digestion with the restriction enzyme PstI. The 2.9 kb ΦX duplex fragment used in the experiment in Figure 4B was generated from a triple digest of the replicative form with PstI, AatII, and StuI. After electrophoresis in a 0.9% agarose gel run in TAE buffer (20 mM Tris–acetate [pH 7.4], 2 mM EDTA), the gel slice containing the 2.9 kb PstI–AatII fragment was dissolved in sodium iodide and purified using the GeneClean kit purchased from BIO 101. Replicative form M13mp18 DNA and h.M13.1 DNA were linearized by treatment with BspHI. All the DNA substrates were stored in TE buffer (10 mM Tris–HCl [pH 7.2], 0.2 mM EDTA).

Standard Pairing and Strand Exchange Reaction Protocol

To assemble the reaction mixture (12.5 μl in final volume), we incubated 5.5 μg of RAD51 protein (10.2 μM) added in 1.2 μl with 120 ng of ΦX174 viral (+) strand (29.5 μM nucleotides) for 5 min at 37°C in 9.5 μl of buffer R (40 mM potassium MES [pH 6.5], 4 mM $MgCl_2$, 100 μg/ml bovine serum albumin, 1 mM DTT, and 2.5 mM ATP), followed by the addition of 1.5 μg RPA (1 μM) in 1 μl and a 10 min incubation at 37°C, and, finally, 120 ng of PstI-linearized ΦX dsDNA (14.75 μM base pairs) in 1 μl and 1 μl of 200 mM $MgCl_2$ were incorporated. After incubation at 37°C for the indicated times, SDS and proteinase K were added to 0.5% and 0.5 mg/ml, respectively, followed by a 15 min incubation at 37°C. The deproteinized samples were mixed with 3 μl of 0.1% orange G in 50% glycerol and loaded on 0.9% agarose gels prepared in TAE buffer (40 mM Tris–acetate [pH 7.5], 0.5 mM EDTA). Electrophoresis was for 15 hr at 1.2 V/cm and 25°C. After being soaked in a large volume of water containing 1 μg/ml ethidium bromide for 90 min to stain DNA, gels were rocked in 1 liter of water for 3–5 hr to reduce background staining. The gels were then placed on a ultraviolet light box and photographed through a red filter with the use of Polaroid type 55 films. For reactions that contained M13 DNAs as substrates, unless stated otherwise, the same amount of viral (+) strand and linear dsDNA as ΦX174 DNAs were used, and the reaction mixture was assembled in the same fashion.

Examination of the Functional Relevance of RAD51-dsDNA Filament

In the experiment described in Figure 4A, the reaction mixture (16.2 μl in final volume) was assembled by incubating 120 ng of ΦX viral (+) strand DNA (22.7 μM nucleotides) with 5.5 μg of RAD51 protein (7.8 μM) and 1.5 μg of RPA (0.77 μM) in 9.5 μl buffer R exactly as described in the standard protocol and then mixing with 1.2 μl of 200 mM $MgCl_2$ and 120 ng of dsDNA (11.35 μM base pairs) that had been preincubated with the indicated amounts of RAD51 for 15 min at 37°C in 4.5 μl of buffer R. After incubation at 37°C, reaction samples were deproteinized and subjected to agarose gel electrophoresis. In the experiment described in Figure 4B, the reaction mixture (17.3 μl in final volume) was assembled by incubating 120 ng of ΦX viral (+) strand (21.3 μM nucleotides) with 5.5 μg of RAD51 (7.3 μM) and 1.5 μg of RPA (0.72 μM) in 9.5 μl buffer R exactly as described in the standard protocol and then mixing with 1.3 μl of 200 mM $MgCl_2$ and 5.5 μl of buffer R containing 90 ng of the full-length linear duplex (8 μM base pairs) and 50 ng of the 2.9 kb linear duplex (4.4 μM base pairs). Alternatively, the RAD51–ssDNA nucleoprotein filament was mixed with 1.3 μl of 200 mM $MgCl_2$, 1 μl of buffer R containing either the full-length linear duplex or the 2.9 kb linear duplex, and 4.5 μl of buffer R containing either the full-length duplex or the 2.9 kb duplex that had been precoated with RAD51 at 2.5 bp per protein monomer at 37°C for 15 min. After incubation at 37°C, reaction samples were deproteinized and subjected to agarose gel electrophoresis. The increased number (~1.5 times of that in the standard reaction) of total long and short duplex DNA molecules used in this experiment did not affect the strand exchange reaction significantly.

Examination of Reaction Polarity

Replicative form h.M13.1 linearized with BspHI was treated with calf intestinal phosphatase to remove the 5′ end phosphate and then labeled with [γ-^{32}P]ATP and T4 polynucleotide kinase. For examining which end of the (−) strand in the labeled dsDNA is utilized in pairing, the reaction mixture (12.5 μl in final volume) was assembled by incubating 120 ng M13mp18 viral (+) strand (29.5 μM nucleotides) with 5.5 μg of RAD51 protein (10.2 μM) and 1.5 μg of RPA (1 μM) exactly as described in the standard protocol and then mixing with 1 μl of 200 mM $MgCl_2$ and 50 ng of the ^{32}P-labeled linear dsDNA (6.1 μM base pairs) in 1 μl. The complete reaction mixture was incubated at 37°C, and at 40, 80, and 120 min, a 2.5 μl aliquot was withdrawn and digested with 10 U of either ClaI (Boehringer Mannheim) or XmnI (New England Biolabs) at 37°C for 5 min in a final volume of 12.5 μl of the buffers supplied by the vendors. Samples were deproteinized and run in 1% agarose gels in TAE buffer for 12 hr at 1.2 V/cm and 25 °C, along with nonradioactive DNA size standards. Gels were stained with ethidium bromide, dried onto a sheet of Whatman 3MM paper, and then exposed to X-ray films to reveal the radioactive bands.

Electron Microscopy

To form RAD51 filaments on ssDNA, we incubated ΦX174 viral (+) strand with RAD51 protein and RPA as described in the standard pairing and strand exchange protocol, except that bovine serum albumin was omitted from the reaction buffer. To form RAD51 filaments on dsDNA, we assembled the reaction mixture by incubating 120 ng of PstI-linearized ΦX174 replicative form DNA (19.4 μM base pairs) with 3.8 μg of RAD51 (9.2 μM) at 37°C for 15 min in 9.5 μl of reaction buffer that lacked bovine serum albumin. The reaction mixtures were diluted 50-fold with ice-cold reaction buffer without bovine serum albumin, applied directly onto polylysine-coated carbon parlodion films on 200 mesh copper grids, and processed to be shadowed with Pt:Pd (80:20) or for negative staining with 1% uranyl acetate as described elsewhere (Flory et al., 1984). The Williams polylysine technique (Williams, 1977), as described by Flory et al. (1984), was further modified by the use of poly-D-lysine (M_r 7 × 10^4 Da; purchased from Sigma; D. L. R. and D. L. Vizard, unpublished data). Grids were examined in either Philips 300 or 410 electron microscope. Magnification was calibrated with a germanium replica of a diffraction grating (54,864 lines per inch; Ladd Industries) also mounted on a 200 mesh copper grid. Length measurements were obtained from tracings of projected images using a map measure. Measurements of nucleofilament parameters were obtained on negatives using a micrometer eyepiece (Bausch and Lomb), and the helical sense was determined by examination of stereopairs of the micrographs.

Densitometry

Images of DNA bands on photographic negatives were analyzed using the Bio-Image system from Millipore to obtain datapoints for graphical presentation of the results.

Acknowledgments

Correspondence should be addressed to P. S. We thank Louise Prakash, Satya Prakash, and Scott Lauder for reading the manuscript and for many helpful suggestions. P. S. gratefully acknowledges Louise Prakash and Satya Prakash for advice and support. D. L. R. wishes to thank Janet Schildmeijer Robberson and Joel Newsome for assistance in electron micrograph measurements and print preparation. This work was supported by National Institutes of Health grant R01-ES07061 (to P. S.) and by the Sealy Center for Molecular Science.

Received May 23, 1995; revised June 29, 1995.

References

Aboussekhra, A., Chanet, R., Adjiri, A., and Fabre, F. (1992). Semidominant suppressors of Srs2 helicase mutations of *Saccharomyces cerevisiae* map in the *RAD51* gene, whose sequence predicts a protein with similarities to procaryotic RecA proteins. Mol. Cell. Biol. *12*, 3224–3234.

Basile, G., Aker, M., and Mortimer, R. K. (1992). Nucleotide sequence

and transcriptional regulation of the yeast recombinational repair gene *RAD51*. Mol. Cell. Biol. *12*, 3235–3246.

Bezzubova, O., Shinohara, A., Mueller, R. G., Ogawa, H., and Buerstedde, J. M. (1993). A chicken RAD51 homologue is expressed at high levels in lymphoid and reproductive organs. Nucl. Acids Res. *21*, 1577–1580.

Bishop, D. K. (1994). RecA homologs Dmc1 and Rad51 interact to form multiple nuclear complexes prior to meiotic chromosome synapsis. Cell *79*, 1081–1092.

Bishop, D. K., Park, D., Xu, L., and Kleckner, N. (1992). *DMC1*: a meiosis-specific yeast homolog of E. coli *recA* required for recombination, synaptonemal complex formation, and cell cycle progression. Cell *69*, 439–456.

Brill, S. J., and Stillman, B. (1989). Yeast replication factor-A functions in the unwinding of the SV40 origin of DNA replication. Nature *342*, 92–95.

Cao, L., Alani, E., and Kleckner, N. (1990). A pathway for generation and processing of double-strand breaks during meiotic recombination in S. cerevisiae. Cell *61*, 1089–1101.

Emery, H. S., Schild, D., Kellogg, D. E., and Mortimer, R. K. (1991). Sequence of *RAD54* , a *Saccharomyces cerevisiae* gene involved in recombination and repair. Gene *104*, 103–109.

Flory, J., Tsang, S. S., and Muniyappa, K. (1984). Isolation and visualization of active pre-synaptic filaments of RecA protein and single-stranded DNA. Proc. Natl. Acad. Sci. USA *81*, 7026–7030.

Griffith, J. D., and Harris, L. D. (1988). DNA strand exchanges. CRC Crit. Rev. Biochem. *23*, S43–S86.

Kmiec, E. B., and Holloman, W. K. (1983). Heteroduplex formation and polarity during strand transfer promoted by Ustilago Rec1 protein. Cell *33*, 857–864.

Kowalczykowski, S. C., Dixon, D. A., Eggleston, A. K., Lauder, S. D., and Rehrauer, W. M. (1994). Biochemistry of homologous recombination in *E. coli*. Microbiol. Rev. *58*, 401–465.

Lovett, S. T. (1994). Sequence of the *RAD55* gene of *Saccharomyces cerevisiae*: similarity of RAD55 to prokaryotic RecA and other RecA-like proteins. Gene *142*, 103–106.

Lovett, S. T., and Mortimer, R. K. (1987). Characterization of null mutants of the *RAD55* gene of *Saccharomyces cerevisiae*: effects of temperature, osmotic strength, and mating type. Genetics *116*, 547–553.

Morita, T., Yoshimura, Y., Yamamoto, A., Murata, K., Mori, M., Yamamoto, H., and Matsushiro, A. (1993). A mouse homolog of the *Escherichia coli recA* and *Saccharomyces cerevisiae RAD51* genes. Proc. Natl. Acad. Sci. USA *90*, 6577–6580.

Ogawa, T., Yu, X., Shinohara, A., and Egelman, E. H.. (1993). Similarity of the yeast RAD51 filament to the bacterial RecA filament. Science *259*, 1896–1899.

Petes T. D., Malone, R. E., and Symington, L. S. (1991). Recombination in yeast. In The Molecular and Cellular Biology of the Yeast *Saccharomyces*: Genome Dynamics, Protein Synthesis, and Energetics, J. R. Broach, J. R. Pringle, and E. W. Jones, eds. (Cold Spring Harbor, New York: Cold Spring Harbor Laboratory Press), pp. 407–521.

Radding, C. M. (1991). Helical interactions in homologous pairing and strand exchange driven by RecA protein. J. Biol. Chem. *266*, 5355–5358.

Roca, A. I., and Cox, M. M. (1990). The RecA protein: structure and function. Crit. Rev. Biochem. Mol. Biol. *25*, 415–456.

Shinohara, A., Ogawa, H., and Ogawa, T. (1992). RAD51 protein involved in repair and recombination in S. cerevisiae is a RecA-like protein. Cell *69*, 457–470.

Shinohara, A., Ogawa, H., Matsuda, Y., Ushio, N., Ikeo, K., and Ogawa, T. (1993). Cloning of human, mouse and fission yeast recombination genes homologous to *RAD51* and *recA*. Nature Genet. *4*, 239–243.

Sun, H., Treco, D., Schultes, N. P., and Szostak, J. W. (1989). Double-strand breaks at an initiation site for meiotic gene conversion. Nature *338*, 87–90.

Sun, H., Treco, D., and Szostak, J. W. (1991). Extensive 3'-overhanging, single-stranded DNA associated with the meiosis-specific double-strand breaks at the *ARG4* recombination initiation site. Cell *64*, 1155–1161.

Sung, P. (1994). Catalysis of ATP-dependent homologous DNA pairing and strand exchange by yeast RAD51 protein. Science *265*, 1241–1243.

Williams, R. C. (1977). Use of polylysine for adsorption of nucleic acids and enzymes to electron microscope specimen films. Proc. Natl. Acad. Sci. USA *74*, 2311–2315.

Yoshimura, Y., Morita, T., Yamamoto, A., and Matsushiro, A. (1993). Cloning and sequence of the human RecA-like gene cDNA. Nucl. Acids Res. *21*, 1665.